AIP | The Journal of Chemical Physics

Evolution of the vibrational spectra of doped hydrogen clusters with pressure

Ruben Santamaria, Jacques Soullard, Xim Bokhimi, and Paulina R. Martínez-Alanis

Citation: The Journal of Chemical Physics **140**, 194301 (2014); doi: 10.1063/1.4875348
View online: http://dx.doi.org/10.1063/1.4875348
View Table of Contents: http://scitation.aip.org/content/aip/journal/jcp/140/19?ver=pdfcov
Published by the AIP Publishing

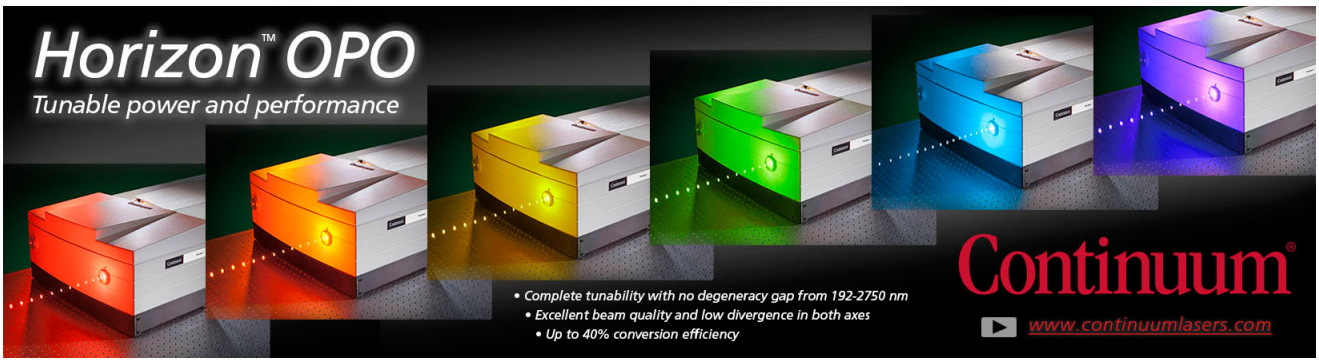

Evolution of the vibrational spectra of doped hydrogen clusters with pressure

Ruben Santamaria,[1,a)] Jacques Soullard,[2] Xim Bokhimi,[2] and Paulina R. Martínez-Alanis[3]
[1]*Department of Chemistry and Biochemistry, University of Arizona, Tucson, Arizona 85721-0041, USA*
[2]*Instituto de Física, UNAM, A.P. 20-364, México D.F., Mexico*
[3]*Instituto de Investigaciones en Materiales, UNAM, A.P. 20-364, México D.F., Mexico*

(Received 4 December 2013; accepted 25 April 2014; published online 15 May 2014)

The evolution of the vibrational spectra of the isoelectronic hydrogen clusters H_{26}, $H_{24}He$, and $H_{24}Li^+$ is determined with pressure. We establish the vibrational modes with collective character common to the clusters, identify their individual vibrational fingerprints and discuss frequency shifts in the giga-Pascal pressure region. The results are of interest for the identification of doping elements such as inert He and ionic Li^+ in hydrogen under confinement or, conversely, establish the pressure of doped hydrogen when the vibrational spectrum is known. At high pressure, the spectra of the nanoclusters resemble the spectrum of a solid, and the nanoclusters may be considered crystals of nanometer scale. The computations are performed at the gradient-corrected level of density functional theory. The investigation is the first of its kind. © *2014 AIP Publishing LLC*. [http://dx.doi.org/10.1063/1.4875348]

INTRODUCTION

The study of clusters represents a fundamental topic of research for several reasons. For instance, they are understood as the tiny counterparts of extended matter from which the macroscopic properties of the material start building up. But, simultaneously, the clusters have properties of their own, like these of physical and chemical nature that change with the cluster size. In this connection, size is conceived as a new physical variable at the nanoscopic level.

Clearly, in the process of growing the cluster the role of the size fades out and the bulk properties are reproduced.[1] Still, some properties initially observed on clusters persist in the extended solid, these are usually of local nature, like the elasticity between contiguous neighbors. In this respect, the equations of state of a cluster and solid are anticipated to have some common features. However, there are other important characteristics that make clusters unique before reaching large sizes. In the region of small sizes, the clusters may play the role of superatoms. Based on the fact that a collection of bonded atoms produces the redistribution of the individual electron densities, due to the delocalization of the nuclear potential, the clusters can induce closed electron shells, thus simulating an elementary atom of bigger size. Similar to elementary atoms, the addition or subtraction of one electron in the superatom is capable to change the reactivity: one extra electron to the closed shell favors the giving of an electron and the superatom mimics an alkali metal atom, and with one less electron, we have a superatom with large electron affinity simulating a halogen atom. In short, one may visualize nanoclusters as the new entities extending the periodic table for "atom" sizes.

The behavior of nanoclusters also depends of the surrounding environment. When we deal with molecules, it is well known that their chemistry changes in confined spaces.[2] However, contrary to molecules, little is known about their energetics and dynamics under the effects of pressure and temperature. Clearly, this is a missing link between the nanoscopic matter and extended solid in environments different to void space. This work contributes in such a direction by characterizing doped hydrogen clusters under pressure from a vibrational perspective. The characterization provides the frequencies, intensities, normal vibrational modes and classifies the unique vibrational markers for the given confined conditions.[3] We use a general methodology developed for clusters under confinement along several papers.[4–9] By using this methodology, it was found that doped hydrogen clusters reach the metallic state at lower pressures than the pure hydrogen species. In an attempt to go along the same line, we compare here the vibrational spectra of pure hydrogen clusters with the corresponding spectra of doped hydrogen clusters. The study unfolds within the harmonic approximation since the harmonic approach is appropriate at high pressure[10] (qualitatively speaking, a particle has less space to move under high pressure due to the interaction potential that becomes narrower and steeper with pressure, keeping the particle away from the anharmonic region of the potential). The spectroscopic data represents a fingerprint and is of help for the identification of clusters with different composition and in different environments. Also, the vibrational spectroscopy is very sensitive to the molecular structure and the spectroscopic data may be employed to reveal changes of the molecular orientational order, put in evidence phase transitions, or provide information of the intermolecular potential.[11] Yet, the vibrational characterization may be used in reversed order, to discern the pressure when vibrational markers of the encapsulated particles have been previously established.

a)Electronic addresses: rbnsntmr@gmail.com; soullard@fisica.unam.mx; bokhimi@fisica.unam.mx; and inukzuk@gmail.com.

On the experimental side, spectroscopic methods have produced a wealth of relevant data. For instance, the infrared spectra of size-selected neutral clusters $(H_2O)_n$ indicate the onset of crystallization when $n = 275 \pm 25$. For $n = 475 \pm 25$, a characteristic ice band is observed.[12] By using the same spectroscopic technique it has been possible to show that nanocages of protonated water $H^+(H_2O)_n$ are formed when $n \geq 21$.[13,14] The studies point out that such nanoclusters play key roles in the structures of aqueous hydrophobic interfaces. Also, based on infrared spectroscopy, the first solvation shells of $OH^-(H_2O)_n$ and $F^-(H_2O)_n$ were determined.[15] Clearly, the results of such clusters are important for understanding the chemistry of water.

In reference to small systems of particles under confinement, there are investigations focused on the properties of endohedrally confined metal atoms in fullerenes. In particular, vibrational properties have been reported.[16] The spectroscopic methods have elucidated the dynamic behavior of the encaged atom *Ce* in C_{82} in gas phase[17] and when C_{82} is adsorbed on a *Cu* surface.[18] Similarly, infrared spectroscopy has elucidated the photodissociation process of $Si(CO)_n$ aggregates.[19] For encapsulated molecules, the spectroscopic studies have provided information of their properties according to the surroundings (see, for instance, the studies of $H_2@C_{60}$[20] and $H_2O@C_{60}$[21]). When the number of confined molecules increases, infrared spectroscopy shows the building of small stable aggregates that are basic for the formation of larger clusters. The formation of cyclic water hexamer in liquid helium droplets[22] and the cyclic HF pentamer in solid para-hydrogen are two particular cases.[23] On the other hand, high pressure Raman spectroscopy, infrared detection, and x-ray studies have shown that clathrate cages retain small hydrogen clusters in their interiors.[24] By using powder x-ray diffraction and Raman spectroscopy, it has been possible to demonstrate that modification of the synthesis process of clathrate hydrates improves their hydrogen storage capacity.[25]

Finally, there is interesting vibrational information of the hydrogen solid under confinement. A Raman frequency turnover at approximately 30 GPa has been observed. For deuterium, it occurs close to 50 GPa. An infrared frequency turnover was detected at 140 GPa, suggesting a transition from the molecular to the atomic state due to the weakening of hydrogen molecular bonds.[26–29] A similar behavior is expected for hydrogen nanoclusters since the vibrational spectrum of the cluster is strongly correlated with its structure, and the structure changes with the pressure. Still, some differences with respect to the solid are expected due to the finite size of the clusters.

CONFINEMENT MODEL OF FINITE SIZE SYSTEMS

The molecular simulation of a system of particles under the effects of pressure demands the presence of confining walls; however, the atomic structure of the walls makes the molecular simulations computationally expensive. In this regard, alternative approaches have emerged making use of extended Lagrangians to include barostat and thermostat effects through virtual particles. These methods show acceptable results for systems with translational symmetry, like crystals,[30,31] but their application to finite size systems remains questionable. In this work, we assume a confinement cage with atomic structure and interacting with the enclosed particles. For finite size systems, the interaction with the container is simply unavoidable because the container is responsible for the pressure exerted on the enclosed particles.

We apply the *TMoFSS* approach (Thermodynamic Model of Finite Size Systems) developed through a series of works,[4–9] since it has shown flexibility, particularly for hydrogen clusters for which it was possible to establish the equation of state, resulting in excellent agreement with this of the solid obtained experimentally. By using the *TMoFSS* model, we also analyzed the transition from the molecular to the atomic state on hydrogen clusters, the induced metallization with pressure, the role of doping elements, temperature effects, etc. In spite of the fact that the clusters represent the finite size counterpart of the solid, and no comparison with the solid is in principle compulsory, the results using *TMoFSS* have shown good agreement with experimental measurements on the solid.

The isoelectronic series to deal with is $H_{24}X$, where $X = H_2, He, Li^+$. It is of interest since the electronic charge spatially spreads according to the number and positions of the positive attractors (the protons in our case). For instance, the electronic charge is spatially delocalized in H_2, but localized in He. On the other hand, in going from He to the ionic element Li^+, mass effects in combination with the effects of adding one more attractor appear. The vibrational spectroscopy is sufficiently sensitive to the rearrangement of the electron cloud and, thereby, permits to identify changes with doping elements. On the other hand, a spherical fullerene conformed by 60 hydrogen atoms plays the role of the container. It is characterized by the radius R_c, and the atoms of the container interact with the encapsulated atoms. By radially shrinking the cage, it is possible to produce different pressures on the confined atoms. Our reference system in the evaluation of doping effects is the cluster H_{26} (i.e., $H_{24}X$ with $X = H_2$). The number of 13 hydrogen molecules is a magic number (Ref. 32) and has shown to be energetically stable at high pressures,[8] with the capacity to provide results compatible with experiments on the solid.[9] Interestingly, the confinement model has put in evidence the self-assemble of hydrogen clusters of different sizes and geometries under extreme pressures.[5]

The imprisoned cluster is energetically optimized for fixed cage atoms. The energy of the cluster is computed by subtracting the energy of the empty H_{60} cage from the energy of the cluster-plus-cage system $H_{24}X@H_{60}$ for fixed cage atoms. The energy of the confined cluster $H_{24}X$ is corrected with zero-point energy effects. In order to classify the thermodynamic state of the confined system, the pressure and volume are determined from a plot of the cluster energy versus the cluster volume. In fact, we make a fit of the plotted data to obtain an analytical function of the type $E = E(V)$. The pressure is determined by differentiation, $P = -(\partial E/\partial V)$. In essence, this constitutes the *TMoFSS* approach, with a computational expense that is not prohibitive, specially for small and medium sized particle systems. The details of the *TMoFSS* approximation can be found elsewhere.[4–9]

METHOD

A true equilibrium geometry of the encapsulated system is obtained when it is energetically relaxed and all the vibrational frequencies are real. To do this, the generalized gradient version of the *DFT* method has shown to be accurate enough to produce energy minima with real vibrational frequencies, particularly for ionic hydrogen clusters.[33] Thus, we use the generalized gradient version of *DFT* with the expressions of Becke for exchange[34] and Lee-Yang-Parr for correlation[35] because these functionals have shown the correct behavior and accuracy in the closing of the energy gap, the building of the equation of state, the Lidemann criterion factor, etc. The calculations are performed with closed shells, as they allow charge mixing between the imprisoned particles and cage atoms with the pressure[5] and present reduced spin contamination. The basis sets are Gaussians $6-31G^*$, they are acceptable to find energy minima with real vibrational frequencies, providing an equation of state close to the experimental one, and low computational cost. Finally, the dispersion forces play important roles in the calculation of binding energies, even for endohedral guests encapsulated in fullerene cages.[36] In our case, the dispersion forces are neglected due to the fact that the clusters under pressure completely fill the inner region of the fullerene and there are no long-range interactions in the interior of the cage.

The electron wave function in the *DFT* method is described by a single determinant of molecular orbitals. The orbitals are determined by self-consistently solving the *DFT* Kohn-Sham one-electron equations. The numerical self-consistent approach is finished when the convergence is 10^{-6} a.u. in both the density matrix and energy. The total energy of the cage-cluster system is minimized over the positions of the encapsulated atoms using the quasi-Newton method.[37] The calculations are performed with the lowest spin multiplicity. The first part of the calculations is performed with the NWChem program.[38] The hydrogen cluster (with no doping element) results with a central H_2 molecule. In the doped clusters, the central H_2 molecule of the previous calculation is replaced by an He or Li^+ impurity, proceeding with the corresponding optimization process from this initial structure. Subsequent to the energy minimization process, a constrained vibrational frequency analysis of the imprisoned particles is done with the cage atoms fixed at their positions. The thresholds in this case are 1.5×10^{-5} hartree/bohr in the maximum force, and 10^{-5} in the root mean square of the force. The constrained vibrational frequency analysis provides the zero-point vibration energy of the confined structure under study. The software package used in this last stage is Gaussian.[39] The computations are performed in a *PC*-cluster. Interestingly, the confinement model is compatible with the new computing technologies and paradigms discussed in Ref. 40.

RESULTS AND DISCUSSION

Vibrational spectrum behavior with pressure

The equation of state that provides the pressure of the clusters was computed in Ref. 9. It is given in the form

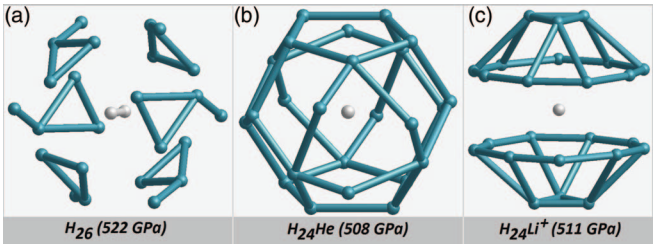

FIG. 1. The pressurized structures of the hydrogen cluster H_{26} and doped clusters $H_{24}He$ and $H_{24}Li^+$ are shown. The pressures are written in parenthesis and correspond to a fullerene cage radius of $R_c = 2.60$ Å (the fullerene cage is omitted for simplicity). The cluster H_{26} (inset (a)) may be visualized as composed by 6 subunits with 4 atoms each one. In cluster $H_{24}He$ (inset (b)), the He atom appears totally encaged while in cluster $H_{24}Li^+$ (inset (c)), the Li^+ ion is partially encaged.

$P = -\partial E_{clu}/\partial V$, where the energy of the cluster is:

$$E_{clu} = a + b\exp(\alpha V^{1/3}) + cV^{1/3}\exp(\alpha V^{1/3}).$$

The confinement volume is V. The parameters (a, b, c, α) have values $(-0.546662, -532.135, 409.019, -3.8778)$ for H_{26}, $(-0.658921, 11.0543, 0.0345819, -2.15142)$ for $H_{24}He$, and $(-0.826997, -65.6111, 72.7757, -3.16335)$ for $H_{24}Li^+$. Figure 1 shows some of the cluster structures. The structures of the pure and doped hydrogen clusters are different under similar pressure conditions (in the neighborhood of 510 GPa). On the other hand, Figure 2 shows the closest-neighbor distance of every atom conforming the cluster. The distances are sufficiently similar that is difficult to discriminate the cluster structures based on these types of plots solely. On the other hand, the vibrational spectra of the isoelectronic series H_{26}, $H_{24}He$ and $H_{24}Li^+$ under different pressures are depicted in the insets of Figures 3(a)–3(c), respectively. The vibrational spectrum changes with the pressure and doping element. With the exception of the highest frequencies

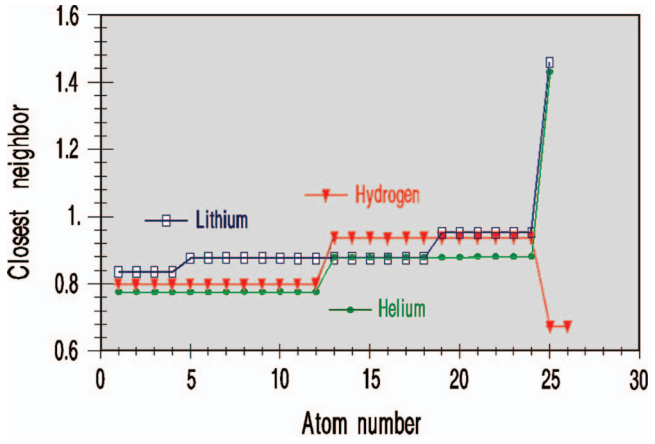

FIG. 2. The plots exhibit the closest-neighbor distance of every atom in the clusters H_{26}, $H_{24}He$ and $H_{24}Li^+$ (shown in in Figure 1). In the case of the clusters H_{26} and $H_{24}He$, we essentially observe 2 plateaus, though the plateaus of the cluster $H_{24}He$ appear closer to each other. The large jumps at the end of these two plots refer to the two central hydrogen atoms in H_{26} and to the He atom in $H_{24}He$. On the other hand, the cluster doped with lithium shows 3 plateaus, some of the plateaus overlap with these of the other clusters. The different plateaus among the clusters are indicative of different structures of the clusters, unfortunately, they are not unique to be considered fingerprints.

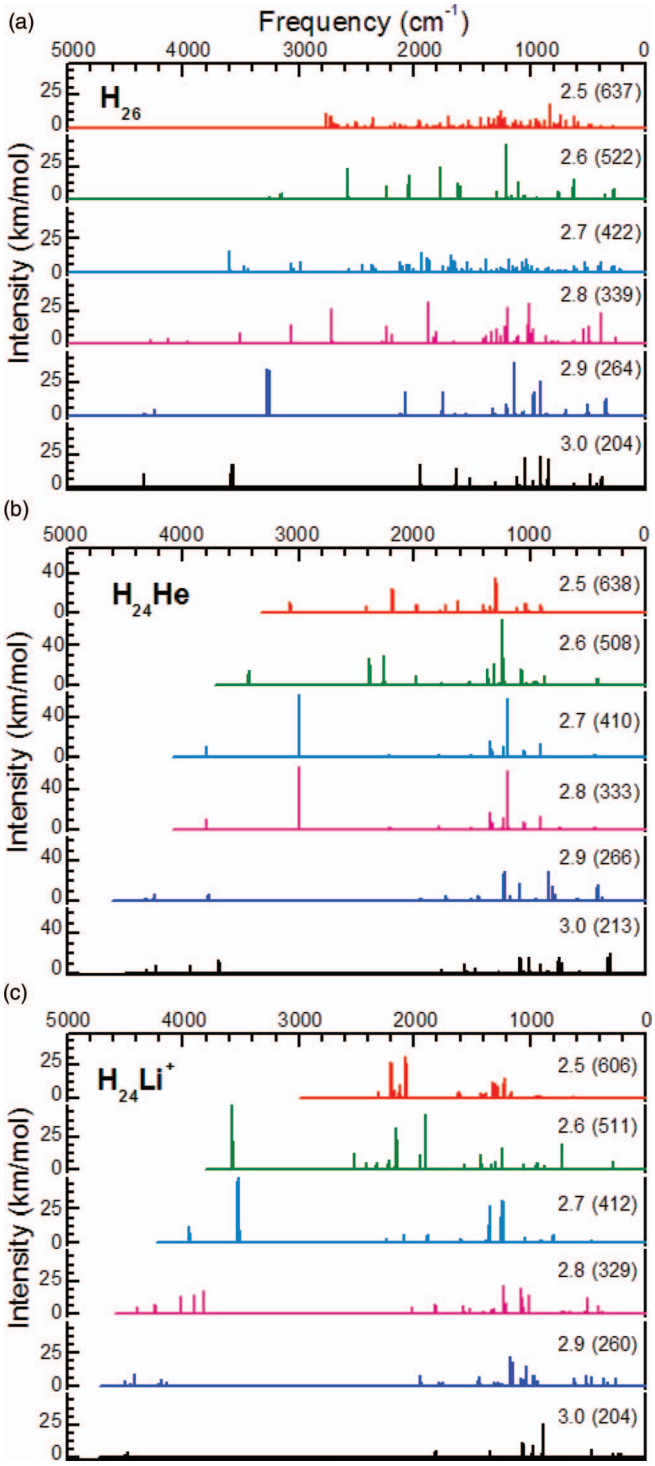

FIG. 3. The harmonic vibrational spectra of the isoelectronic clusters H_{26}, $H_{24}He$ and $H_{24}Li^+$ under confinement are presented for some selected pressures and frequencies lower than 5000 cm^{-1}. The numbers in the insets are the cage radii R_c (Å) and in parenthesis the corresponding pressures (GPa). The vibrational spectra change with both the pressure and doping element.

(these are discussed below), a narrowing process of the vibrational spectrum is observed when the pressure increases. In particular, the spectrum of H_{26} exhibits closely packed frequencies and more similar intensities. This behavior is compatible with that shown in Ref. 11 for the D_2 overtone, temperature 77 K. The number of frequencies of the cluster remains constant since the degrees of freedom are not changed in the process of increasing the pressure. The behavior of the H_{26} spectrum is associated with a conformation evolving towards a more symmetric structure with pressure. In the limit of very high pressures, we expect frequencies with much closer values, and since the number of frequencies is always preserved, vibrational degeneracy should start to emerge. However, the vibrational degeneracy of the cluster should be distinguished from this of the solid. In the cluster case, the pressure induces higher spatial symmetry, leading to the degeneracy of vibrational frequencies, while the vibrational degeneracy of the hydrogen solid is dominated by a periodic structure, observable at any pressure regime, with an upper bound established by the crystal Debye frequency. The conclusion is that clusters without pressure may play the role of superatoms, but under the effects of high pressure they reveal vibrational properties like these of extended solids due to the vibrational degeneracy induced by the pressure.

A similar compact behavior of the spectrum is observed in doped hydrogen clusters. The individual vibrational markers of He and Li^+ are distinguished in the spectra of $H_{24}He$ and $H_{24}Li^+$, becoming more pronounced in the high pressure region (further discussion is provided later).

Analysis of vibrational frequencies

The highest and smallest vibration frequencies of the isoelectronic clusters H_{26}, $H_{24}He$ and $H_{24}Li^+$ are shown in Table I in terms of the pressure. The highest frequencies of H_{26} are assigned to bond stretching of the central H_2 molecule and essentially increase when the pressure increases. The doped systems exhibit monotonic reduction of the highest frequencies by increasing the pressure. In this case, the normal modes exclude the doping elements, but involve coplanar hydrogens. The hydrogen planes vibrate towards each other (as opposed to molecules, where we usually observe no-vibrating planes). The monotonic reduction of frequencies is attributed to a localized nuclear potential. More precisely, in the pure hydrogen H_{26} case, we have a delocalized nuclear potential at the cluster core, but a localized potential in the $H_{24}He$ and $H_{24}Li^+$ cases.

In reference to the smallest frequency of the isoelectronic clusters H_{26}, $H_{24}He$ and $H_{24}Li^+$, there are mixed behaviors (decreasing and increasing variations) when the pressure increases. The most irregular behavior is given by H_{26}. From

TABLE I. Highest and smallest vibrational frequencies ν of the isoelectronic clusters H_{26}, $H_{24}He$ and $H_{24}Li^+$ according to the pressure and cage radius R_c.

	Pressure (GPa)			Highest ν (cm^{-1})			Smallest ν (cm^{-1})		
R_c (Å)	H_{26}	$H_{24}He$	$H_{24}Li^+$	H_{26}	$H_{24}He$	$H_{24}Li^+$	H_{26}	$H_{24}He$	$H_{24}Li^+$
3.00	204	213	204	5052	4485	4530	221	139	166
2.90	264	266	260	5074	4416	4516	163	224	196
2.80	339	333	329	5144	4320	4391	136	224	260
2.70	422	410	412	5250	3885	4028	221	330	284
2.60	522	508	511	5388	3531	3610	272	403	284
2.50	637	638	606	5381	3137	2797	97	345	391

204 up to 339 GPa the smallest frequency keeps reducing, but at 422 GPa the reduction pattern is inverted. The change exposes a frequency turnover between 339 and 422 GPa for the smallest frequency. It is associated to structural changes of the cluster with the pressure. On the other hand, the smallest frequencies of the clusters $H_{24}He$ and $H_{24}Li^+$ increase when the pressure is increased (from ∼210 up to ∼510 GPa). It is in the region of very high pressure (∼600 GPa) that the smallest frequencies of H_{26} and $H_{24}He$ are inverted. At such high pressures, the atoms conforming the cage strongly interact with the encapsulated atoms, and the turnover points in this interval may be not uniquely associated to the cluster. In the case of $H_{24}Li^+$, a monotonic behavior is obtained in the pressure interval explored, nevertheless, a soft turnover appears between 412 and 511 GPa. For the case of the $H_{24}He$ cluster, the soft turnover occurs at 224 GPa.

The pressure exerted on doped hydrogen clusters produces a more compact vibrational spectra. This is not the case for the pure hydrogen cluster. The vibrational degeneracy of the clusters, resembling that of a crystal, starts to appear in the high pressure limit. Thus, the clusters are expected to exhibit the properties of a crystal under equal conditions of pressure. In some sense, this property complements the discussion presented in the introductory section: a cluster may play the role of a nanosize atom (superatom) at very low pressures, while it may play the role of a nanocrystal at high pressures. Also, we found frequency turnover points for all the isoelectronic clusters at different pressures, but they appear for the smallest frequencies, not for the highest ones. The frequency turnover points are associated to structural changes with the pressure. In the following sections, we clarify the observations by analyzing vibrational modes in different spectral regions.

Vibrational modes

The computation of the vibrations of the three isoelectronic clusters under different pressures provides a vast spectroscopic data (an minimum of 75 vibrational modes of each cluster, with computations for six different pressures). In this regard, it is convenient to pay attention to the most representative vibrational modes. To do this, we discuss modes showing similar vibrational patterns and others that classify individually.

Vibrations with breathing character

The breathing modes are relatively easy to identify and are important among the collective vibrations. The breathing modes are observed in the three cluster species, but with different frequencies due to the doping elements and the pressure exerted over the clusters. In order to measure the breathing of the mth mode, we define the breathing character bc^m:

$$bc^m = (1/N)\sum_{i=1}^{N} \mathbf{q}_i^m \cdot \mathbf{r}_i / \left(\left|\mathbf{q}_i^m\right| |\mathbf{r}_i|\right), \qquad (1)$$

where $\mathbf{r}_i/|\mathbf{r}_i|$ is the unit vector position of the ith atom, $\mathbf{q}_i^m/|\mathbf{q}_i^m|$ the unit vibration vector of such an atom in the mth mode, and N is the number of active atoms vibrating in the cluster. In our case, $N = 26$ for the pure hydrogen cluster and 24 for the doped hydrogen clusters. The dot products are introduced to project the vibrational mode along the radial direction. In some instances, such products may be positive or negative, indicative of atoms vibrating in different radial directions. A pure breathing of the cluster is achieved when all atoms move radially in the same direction. For the case of H_{26}, we denote the pure breathing mode in the form (26, 0) or (0, 26) to indicate that all atoms (26 in total) move either in the negative or positive radial directions, respectively. The vibrations with less breathing character are denoted similarly, for example, the term (10, 16) indicates that 10 atoms move in the negative radial direction but the other 16 move in the positive direction. On the other hand, the term (13, 12) points out that 25 atoms vibrate, 13 in one direction, 12 on the opposite one and one additional atom contributes with zero dot product (for instance, static atoms have $\mathbf{q}_i^m = 0$, or when an atom is located at the origin $\mathbf{r}_i = 0$). For a given breathing mode, the positive or negative signs of the radial directions simply represent a phase factor and are of secondary importance here. In Table II, we show the first three vibrational modes with highest breathing character under different pressures. The magnitude of the breathing character (bc) is given there. A pure breathing vibrational mode acquires the value $bc^m = 1$, while vibrations with smaller values indicate non-pure breathing character.

Table II shows that none of the vibrations are pure breathing modes, making the bc numbers lower than 1.0 (but many of them with values above 0.9). In the case of H_{26}, the vibrational frequency increases when the pressure is increased. Small bc numbers appear at pressures 422 and 339 GPa. According to our previous investigations, this is the pressure range where metalization and atomization of the hydrogen cluster show up.[6] Other vibrations of H_{26} also exhibit breathing character but their bc numbers are substantially lower with respect to these of doped clusters. In the low pressure region, the frequencies of the doped clusters are relatively close to the frequencies of H_{26}; however, the differences become slightly more pronounced in the high pressure region. In the pressure range $410 - 638$ GPa, the bc numbers of $H_{24}He$ deteriorate and, for $H_{24}Li^+$, it occurs in the pressure range $412 - 511$ GPa.

Vibrational fingerprints of the confined clusters

We are interested in identifying the vibrational fingerprints of the clusters. The pure hydrogen cluster H_{26} contains a central H_2 molecule plus 24 hydrogen atoms surrounding it (see Figure 1). The central H_2 molecule is a distinctive component and any vibration where it takes significant part constitutes a vibrational marker of H_{26}. The vibrations of the central molecule change with the pressure, nevertheless, it is possible to classify them in four categories. Two of these involve static mass centers of the central molecule, and the other two non-static mass centers. In the case of the static centers of mass (CM), the H_2 molecule may present stretching vibration or quasi-rotation of the molecular bond with fixed CM. In the case of non-static CM, the central molecule exhibits translating motion that may be parallel or perpendicular to the H_2

TABLE II. Vibrational modes with large breathing character of the isoelectronic confined clusters H_{26}, $H_{24}He$ and $H_{24}Li^+$ according to the pressure.[a]

H_{26}

P=204 (R_c=3.00)		P=264 (R_c=2.90)		P=339 (R_c=2.80)	
ν	Mag. (−, +)	ν	Mag. (−, +)	ν	Mag. (−, +)
1954	0.915 (0,25)	2089	0.941 (0,26)	2200	0.749 (0,26)
1602	0.203 (10,16)	1727	0.248 (20,6)	2290	0.526 (23,3)
1295	0.163 (18,8)	1326	0.218 (18,8)	1875	0.267 (6,20)
P=422 (R_c=2.70)		P=522 (R_c=2.60)		P=637 (R_c=2.50)	
ν	Mag. (−, +)	ν	Mag. (−, +)	ν	Mag. (−, +)
2230	0.619 (25,1)	2405	0.907 (26,0)	2799	0.935 (26,0)
2041	0.397 (21,5)	3077	0.441 (24,2)	5381	0.219 (7,14)
3043	0.329 (21,5)	1383	0.214 (13,12)	1501	0.180 (10,16)

$H_{24}He$

P=213 (R_c=3.00)		P=266 (R_c=2.90)		P=333 (R_c=2.80)	
ν	Mag. (−, +)	ν	Mag. (−, +)	ν	Mag. (−, +)
1959	0.975 (0,24)	2106	0.987 (0,24)	2248	0.995 (0,24)
1218	0.211 (16,8)	1791	0.161 (12,12)	1451	0.146 (16,8)
3913	0.119 (14,10)	986	0.097 (10,14)	1070	0.124 (10,14)
P=410 (R_c=2.70)		P=508 (R_c=2.60)		P=638 (R_c=2.50)	
ν	Mag. (−, +)	ν	Mag. (−, +)	ν	Mag. (−, +)
2140	0.737 (0,24)	2499	0.891 (24,0)	2498	0.753 (0,24)
2560	0.583 (24,0)	1916	0.322 (22,2)	3078	0.582 (24,0)
1951	0.322 (20,4)	3531	0.182 (12,12)	2306	0.304 (0,24)

$H_{24}Li^+$

P=204 (R_c=3.00)		P=260 (R_c=2.90)		P=329 (R_c=2.80)	
ν	Mag. (−, +)	ν	Mag. (−, +)	ν	Mag. (−, +)
1970	0.981 (0,24)	2104	0.984 (0,24)	2218	0.971 (0,24)
1705	0.275 (12,12)	1823	0.242 (12,12)	1257	0.230 (8,16)
1743	0.207 (8,16)	1849	0.172 (16,8)	1400	0.208 (16,8)
P=412 (R_c=2.70)		P=511 (R_c=2.60)		P=606 (R_c=2.50)	
ν	Mag. (−, +)	ν	Mag. (−, +)	ν	Mag. (−, +)
2224	0.845 (0,24)	2575	0.866 (0,24)	2714	0.981 (0,24)
1948	0.421 (0,24)	2435	0.408 (0,24)	2283	0.237 (8,16)
2945	0.315 (6,18)	2668	0.321 (6,18)	2470	0.200 (8,16)

[a]Frequency ν in cm^{-1}, pressure P in GPa and cage radius R_c in Å. The values in parenthesis are numbers of atoms vibrating in the negative and positive radial directions (as discussed in the body text). The magnitude (Mag.) represents the value of bc^m (displayed in Eq. (1)).

bond. Table III presents the translational modes with largest amplitudes and the quasi-rotational modes with the largest angles of the central H_2 molecule. The dominant translational motions of the H_2 molecule are of perpendicular type and only some modes involve the parallel translational form. The vibrational frequencies of the translational motions increase when the pressure is increased. On the other hand, the largest angles for the quasi-rotational vibrations of H_2 are close to 50°. Surprisingly, the quasi-rotational vibrations come and go with the pressure, at 412 and 606 GPa no quasi-rotational vibrations are observed. Unfortunately, the vibrational frequencies of the quasi-rotational vibrations of H_2 describe no clear pattern with pressure.

In regard to the doped clusters, we are interested in the modes where He and Li^+ vibrate noticeably. In Table IV, we present their fingerprints with pressure and,

TABLE III. Translational and quasi-rotational modes of the central H_2 molecule in the confined cluster H_{26} according to the pressure.[a]

Translational modes

P=204 (R_c=3.00)		P=260 (R_c=2.90)		P=329 (R_c=2.80)	
ν	Dir.	ν	Dir.	ν	Dir.
1232	⊥	2118	⊥	2276	⊥
1228	⊥	2113	⊥	2241	⊥
1981	⊥	1296	⊥	1015	∥
P=412 (R_c=2.70)		P=511 (R_c=2.60)		P=606 (R_c=2.50)	
ν	Dir.	ν	Dir.	ν	Dir.
2389	⊥	816	∥	2691	⊥
2452	⊥	2575	⊥	2721	⊥
2280	∥	2573	⊥	2763	⊥

Quasi-rotational modes

P=204 (R_c=3.00)		P=264 (R_c=2.90)		P=339 (R_c=2.80)	
ν	Angle	ν	Angle	ν	Angle
724	49.4	810	52.1	845	53.8
728	48.8	818	51.6	880	52.0
815	47.0	910	43.8	136	36.3
P=412 (R_c=2.70)		P=511 (R_c=2.60)		P=606 (R_c=2.50)	
ν	Angle	ν	Angle	ν	Angle
...	...	624	49.7	...	...
...	...	613	48.6	...	...
...	...	387	43.1	...	...

[a]Frequency ν in cm^{-1}, pressure P in GPa, cage radius R_c in Å, and angles in degrees. The symbols ⊥ and ∥ indicate perpendicular and parallel translational motion of the H_2 molecule with respect to its bond axis. The horizontal dots indicate that no vibrational mode was identified for the particle in the cluster under the given pressure.

TABLE IV. Vibrational modes of the isoelectronic confined clusters H_{26}, $H_{24}He$ and $H_{24}Li^+$ showing the largest oscillation amplitudes of the central particles H_2, He and Li^+, respectively.[a]

Stretching vibration of H_2 in H_{26}

P=204 (R_c=3.00)	P=264 (R_c=2.90)	P=339 (R_c=2.80)
5052	5074	5144
P=412 (R_c=2.70)	P=511 (R_c=2.60)	P=606 (R_c=2.50)
5250	5388	5381

Oscillation of He in $H_{24}He$

P=204 (R_c=3.00)	P=260 (R_c=2.90)	P=329 (R_c=2.80)
788	842	871
755	841	892
752	808	894
P=412 (R_c=2.70)	P=511 (R_c=2.60)	P=606 (R_c=2.50)
916	944	1001
868	1524	1620
863	1518	1621

Oscillation of Li^+ in $H_{24}Li^+$

P=204 (R_c=3.00)	P=260 (R_c=2.90)	P=329 (R_c=2.80)
516	567	631
510	588	587
529	609	529
P=412 (R_c=2.70)	P=511 (R_c=2.60)	P=606 (R_c=2.50)
585	626	719
635	638	708
627	653	714

[a]Frequency in cm^{-1}, pressure P in GPa, and cage radius R_c in Å.

in addition, the bond stretchings of the central H_2 molecule of H_{26} are included. The frequencies of the bond stretching vibrations of H_2 increase slowly with pressure; however, the oscillations of the doping elements He and Li^+ exhibit bigger changes with pressure.

CONCLUSIONS

We have investigated the evolution of the vibrational spectra of pure and doped hydrogen clusters in the giga-Pascal pressure region. The doping elements are He and Li^+ to conform the isoelectronic cluster series $H_{24}H_2$, $H_{24}He$ and $H_{24}Li^+$. The vibrational spectra becomes more compact when the pressure is increased and, at very high pressure, the spectra resemble this of a solid. In the high pressure region, the clusters are expected to behave like tiny crystals at the nanodimension scale. The doping elements are capable to modify the vibrational spectra of the pure hydrogen cluster by showing their vibrational fingerprints. The whole set of clusters exhibit collective vibrations such as the breathing modes, with frequencies that depend of the doping element and exerted pressure. We observe soft and strong turnovers of the frequency (as it occurs in the solid). In reference to the confinement model, it is sufficiently flexible and accurate that can be applied to other systems of different nature and sizes, and helpful to establish the thermodynamic state of the system under confinement. The importance of this work involves, from a general perspective, the characterization of matter at the nanoscopic level in environments different to void space.

ACKNOWLEDGMENTS

The authors thank the *IFUNAM* and *DGTIC* computer staff for access to Khua and KanBalam *CPU − GPU* clusters.

[1] *Handbook of Nanophysics: Clusters and Fullerenes. Part I: Free Clusters*, edited by K. D. Sattler (CRC Press, London, 2011).
[2] A. M. Rouhi, Chem. Eng. News **78**, 40 (2000).
[3] B. A. Hess, Jr., L. J. Schaad, P. Cársky, and R. Zahradník, Chem. Rev. **86**, 709 (1986).
[4] J. Soullard, R. Santamaria, and S. A. Cruz, Chem. Phys. Lett. **391**, 187 (2004).
[5] R. Santamaría and J. Soullard, Chem. Phys. Lett. **414**, 483 (2005).
[6] J. Soullard, R. Santamaria, and J. Jellinek, J. Chem. Phys. **128**, 064316 (2008).
[7] R. Santamaria, J. Soullard, and J. Jellinek, J. Chem. Phys. **132**, 124505 (2010).
[8] J. Soullard, R. Santamaria, and D. Boyer, J. Phys. Chem. A **115**, 9790 (2011).
[9] R. Santamaria, X. Bokhimi, J. Soullard, and J. Jellinek, J. Phys. Chem. A **117**, 5642 (2013).
[10] R. J. Hemley, H. K. Mao, L. W. Finger, A. P. Jephcoat, R. M. Hazen, and C. S. Zha, Phys. Rev. B **42**, 6458 (1990).
[11] H.-k. Mao and R. J. Hemley, Rev. Mod. Phys. **66**, 671 (1994).
[12] C. C. Pradzynski, R. M. Forck, T. Zeuch, P. Slavíček, and U. Buck, Science **337**, 1529 (2012).
[13] M. Miyazaki, A. Fujii, T. Ebata, and N. Mikami, Science **304**, 1134 (2004).
[14] J.-W. Shin, N. I. Hammer, E. G. Diken, M. A. Johnson, R. S. Walters, T. D. Jaeger, M. A. Duncan, R. A. Christie, and K. D. Jordan, Science **304**, 1137 (2004).
[15] W. H. Robertson, E. G. Diken, E. A. Price, J.-W. Shin, and M. A. Johnson, Science **299**, 1367 (2003).
[16] H. Shinohara, Rep. Prog. Phys. **63**, 843 (2000).
[17] W. Sato, K. Sueki, K. Kikuchi, K. Kobayashi, S. Suzuki, Y. Achiba, H. Nakahara, Y. Ohkubo, F. Ambe, and K. Asai, Phys. Rev. Lett. **80**, 133 (1998).
[18] K. Muthukumar, A. Stróżecka, J. Mysliveček, A. Dybek, T. J. S. Dennis, B. Voigtländer, and J. A. Larsson, J. Phys. Chem. C **117**, 1656 (2013).
[19] A. D. Brathwaite and M. A. Duncan, J. Phys. Chem. A **116**, 1375 (2012).
[20] Y. Kohama, T. Rachi, J. Jing, Z. Li, J. Tang, R. Kumashiro, S. Izumisawa, H. Kawaji, T. Atake, H. Sawa, Y. Murata, K. Komatsu, and K. Tanigaki, Phys. Rev. Lett. **103**, 073001 (2009).
[21] K. Kurotobi and Y. Murata, Science **333**, 613 (2011).
[22] K. Nauta and R. E. Miller, Science **287**, 293 (2000).
[23] Y. Miyamoto, H. Ooe, S. Kuma, K. Kawaguchi, K. Nakajima, I. Nakano, N. Sasao, J. Tang, T. Taniguchi, and M. Yoshimura, J. Phys. Chem. A **115**, 14254 (2011).
[24] W. L. Mao, H.-K. Mao, A. F. Goncharov, V. V. Struzhkin, Q. Guo, J. Hu, J. Shu, R. J. Hemley, M. Somayazulu, and Y. Zhao, Science **297**, 2247 (2002).
[25] R. G. Grim, P. B. Kerkar, M. Shebowich, M. Arias, E. D. Sloan, C. A. Koh, and A. K. Sum, J. Phys. Chem. C **116**, 18557 (2012).
[26] S. K. Sharma, H. K. Mao, and P. M. Bell, Phys. Rev. Lett. **44**, 886 (1980).
[27] R. T. Howie, C. L. Guillaume, T. Scheler, A. F. Goncharov, and E. Gregoryanz, Phys. Rev. Lett. **108**, 125501 (2012).
[28] C.-S. Zha, Z. Liu, and R. J. Hemley, Phys. Rev. Lett. **108**, 146402 (2012).
[29] E. Gregoryanz, A. F. Goncharov, K. Matsuishi, H.-K. Mao, and R. J. Hemley, Phys. Rev. Lett. **90**, 175701 (2003).
[30] S. A. Bonev, E. Schwegler, T. Ogitsu, and G. Galli, Nature (London) **431**, 669 (2004).
[31] H. Kitamura, S. Tsuneyuki, T. Ogitsu, and T. Miyake, Nature (London) **404**, 259 (2000).
[32] J. I. Martínez, M. Isla, and J. A. Alonso, Eur. Phys. J. D **43**, 61 (2007).
[33] L. Huang, C. F. Matta, and L. Massa, J. Phys. Chem. A **115**, 12445 (2011).
[34] A. D. Becke, Phys. Rev. A **38**, 3098 (1988).
[35] C. Lee, W. Yang, and R. G. Parr, Phys. Rev. B **37**, 785 (1988).
[36] P. Pyykkö, C. Wang, M. Straka, and J. Vaara, Phys. Chem. Chem. Phys. **9**, 2954–2958 (2007).
[37] J. Nocedal and S. J. Wright, *Numerical Optimization* (Springer, New York, 1999), Chaps. 8 and 9.
[38] R. J. Harrison *et al.*, High Performance Computational Chemistry Group, NWCHEM, A Computational Chemistry Package for Parallel Computers Version 4.1, Pacific Northwest National Laboratory, Richland, Washington, 2002.
[39] M. J. Frisch, G. W. Trucks, H. B. Schlegel *et al.*, GAUSSIAN 09, Revision A.02, Gaussian, Inc., Wallingford, CT, 2009.
[40] M. S. Friedrichs, P. Eastman, V. Vaidanyathan, M. Houston, S. Legrand, A. L. Beberg, D. Ensign, C. M. Bruns, and V. Pande, J. Comput. Chem. **30**, 864 (2009).